Translational Research in Anatomy 35 (2024) 100290

Contents lists available at ScienceDirect

Translational Research in Anatomy

journal homepage: www.elsevier.com/locate/tria

Unpacking the terminology used in human cochlear dimension methodologies

Rene Human-Baron [a,b,*], Tania Hanekom [b]

[a] Department of Anatomy, School of Medicine, Faculty of Health Sciences, University of Pretoria, Pretoria, 0002, South Africa
[b] Bioengineering, Department of Electrical, Electronic and Computer Engineering, Faculty of Engineering, University of Pretoria, Pretoria, 0002, South Africa

ARTICLE INFO

Keywords:
cochlea
cochlear variation
Dimension
μCT
Terminology

ABSTRACT

Many definitions of the dimensions of cochlear measurements are described in the literature. However, these terminologies are typically not standardised or vary among disciplines. Confusion of the defined parameters may lead to ambiguity in the derived dimensions. Inconsistent terminology may, therefore, contribute to the variations reported in cochlear morphology. This article proposes using a standard set of terminology, including its associated landmarks and measurements, to describe the shape and dimensions of the human cochlea. To provide a basis for comparison for the dimensional description of ambiguous terms in the literature and to supplement existing data where terms are unique, micro-CT (μCT) scans of thirty temporal bones were subjected to landmarking and measuring according to the terminology standard. The results confirm that methodological techniques and definitions of cochlear measurements may affect the quantification of dimensions that describe cochlear morphology and may, therefore, introduce variations when reporting these measurements. Histology and μCT images, for example, could provide a more accurate and comprehensive measure of cochlear dimensions than measurements on casts.

1. Introduction

Person-specific computational models of the implanted cochlea have been applied clinically to investigate complications with cochlear implants (CIs) and to identify possible interventions, e.g., to alleviate facial nerve stimulation [1,2]. Geometric parameters for the computational models are derived from cochlear dimensions obtained from CI recipients' imaging data. The models are, therefore, created from a transdisciplinary fusion of engineering and anatomy. The approach allows the translation of computational models to clinical application, supporting the management of CI recipients' hearing performance within a person-centred care framework. A computational modelling study by Malherbe, Hanekom and Hanekom [3] suggested that variation in cochlear geometry is an important contributor to variations observed in auditory neuron excitation patterns elicited by electrical stimulation with a CI. Neural excitation patterns, in turn, are related to the hearing outcomes that may be achieved with a CI. Within this context, an unambiguous quantitative description of cochlear anatomy and morphology that captures inter-person variations is essential.

The literature describes several dimensions and landmarks to quantify the geometry of the cochlea [4–6], yet standard terminology is lacking. This article explores and explains the terminology applied throughout the literature and proposes consistent terminology. It also reports on the cochlear dimensions described by this terminology as noted in the literature and observed from our study on micro-computed tomography (μCT) images of human cochleae. The article's objective is to provide a standard reference for measuring cochlear dimensions and the typical magnitudes of these dimensions. This reference may serve as a reconstruction and validation scaffold for high-fidelity three-dimensional (3D) computational models of the cochlear geometry, specifically within the context of CI modelling. Low-resolution images, such as those available for live CI recipients' cochleae, tend to underestimate the size of the cochlea [7]. This may have consequences for electrode selection, surgical planning, and the construction of 3D computational models of the cochlea.

2. Materials and methods

2.1. Standardised terminology

Landmark-based quantification of the morphology of the cochlea requires two standards. The first is a set of landmarks that may be used

* Corresponding author. Department of Anatomy, School of Medicine, Faculty of Health Sciences, University of Pretoria, Pretoria, 0002, South Africa.
E-mail addresses: rene.baron@up.ac.za (R. Human-Baron), tania.hanekom@up.ac.za (T. Hanekom).

https://doi.org/10.1016/j.tria.2024.100290
Received 4 January 2024; Received in revised form 13 February 2024; Accepted 13 February 2024
Available online 23 February 2024

to describe the detailed anatomy of the cochlea, and the second is a set of measurement that may be derived from the landmarks to provide a basis for comparison among different imaging modalities, measuring techniques, data sets and observers. A standardised cochlear coordinate system defined in accordance with the standard views of the cochlea and the planes on which each dimension is taken forms the basis for determining standardised measurements.

2.2. The cochlear coordinate system

Variation in measurements may result from the inaccurate alignment of the cochlea with the coordinate system used to obtain the measurements. Verbist, Skinner, Cohen, Leake, James, Boëx, Holden, Finley, Roland, Roland, Haller, Patrick, Jolly, Faltys, Briaire and Frijns [8] proposed a 3D cylindrical cochlear coordinate system having the xy-plane aligned with the base of the cochlea and the z-axis aligned with the modiolus. The alignment of the cochlea to a cartesian coordinate system is shown in Fig. 1. The z-axis is aligned with the modiolar axis (*cochlear height axis*), the x-axis (*cochlear length axis*, also called the *long axis* of the cochlea) is aligned with a plane passing through the centre of the round window and the modiolus while the y-axis (*cochlear width axis*, also called the *short axis* of the cochlea) is perpendicular to the length axis. Consequently, the xz-plane is the *cochlear length plane*, the yz-plane is the *cochlear width plane*, and the xy-plane is the *base plane*.

For modelling purposes, the convention for a left cochlea rotating in a clockwise direction when viewed from the apex, is that a left-handed coordinate system is used, while for a right cochlea, rotating in an anticlockwise direction, a right-handed coordinate system is used. This convention allows for positive angles θ (in the base-to-apex ascending direction of the cochlea) for landmarks in a cylindrical coordinate system. The positive x-axis is at $\theta = 0$. Furthermore, $z = 0$ (the location of the xy or base plane) is chosen such that all height measurements are positive.

A landmark k, as shown in Fig. 1, can be described in the cartesian coordinate system using its (x, y, z) coordinate. The location of the same landmark k can also be defined using cylindrical coordinates, i.e. by its radius r, angle θ, and the height z of the landmark, as shown in Fig. 1 [8].

2.3. The views, planes, and anatomical directions of the cochlea

It is necessary to take note of the different views of the cochlea to interpret the set of measurements used to describe the dimensions and morphology of the cochlea. Furthermore, it is important to realise that different terminologies exist to refer to the views of the cochlea. Anatomical terminology is used for the cochlea while *in situ,* as given in Fig. 2, and radiological and clinical terminology refer to the cochlea *ex vivo*. Radiological terminology is used to describe the anatomical directions of the cochlea relative to its local anatomical structure for imaging purposes, while clinical terminology uses a combination of anatomical and radiological terminology. To appreciate reports originating from different disciplines, it is important to cross-reference terminology among these disciplines.

2.3.1. Round-window view

The *round-window-view* of the cochlea (Fig. 3a) as described by Pietsch, Aguirre Dávila, Erfurt, Avci, Lenarz and Kral [9,10] is viewed from the vestibule perpendicular to the modiolar axis and aligned horizontally through the midpoint of the round window. This view is from positive to negative x along the long axis of the cochlea, perpendicular to the width plane of the cochlea, i.e., it "looks onto" the width plane of the cochlea. The *Pöschls view* is the radiological term for this aspect, while the *axial-pyramidal* or *lateral view* is the anatomical term [4]. Consequently, the *Pöschl projection* is the radiographic projection along the long axis of the petrous bone on a plane parallel to the short axis.

2.3.2. Medial view

The *medial view* (anatomically) of the cochlea (Fig. 3b), also called the *ascending spiral view* [10] is obtained 180° from the round-window view. This view is, therefore, from negative to positive x along the long axis of the cochlea, perpendicular to the width plane of the cochlea.

2.3.3. Side view

A *side view* of the cochlea refers to a view onto the intact cochlea perpendicular to the modiolar axis. The round-window (Fig. 3a) and medial (Fig. 3b) views are special cases of a side view of the cochlea where the view angles are known.

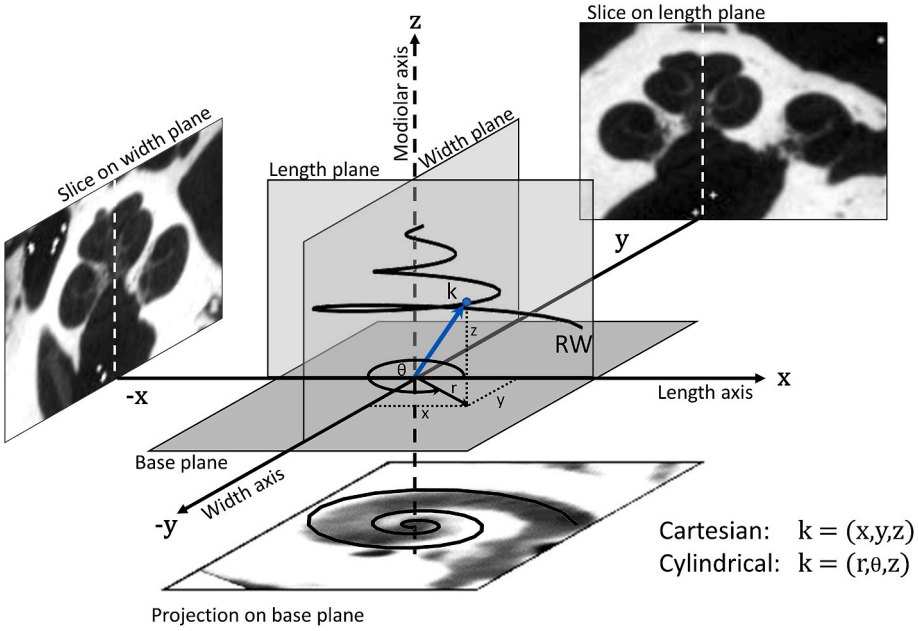

Fig. 1. The cochlear coordinate systems for a right cochlea. The 3D spiral in the centre of the Figure represents the 3D trajectory of a cochlea. Sections through a cochlea (μCT images) are shown on the length and width planes, and a projection of the cochlea is shown on a base plane. The coordinates for landmark k on the cochlear spiral are illustrated for cartesian (x, y, z) and cylindrical (r, θ, z) coordinates.

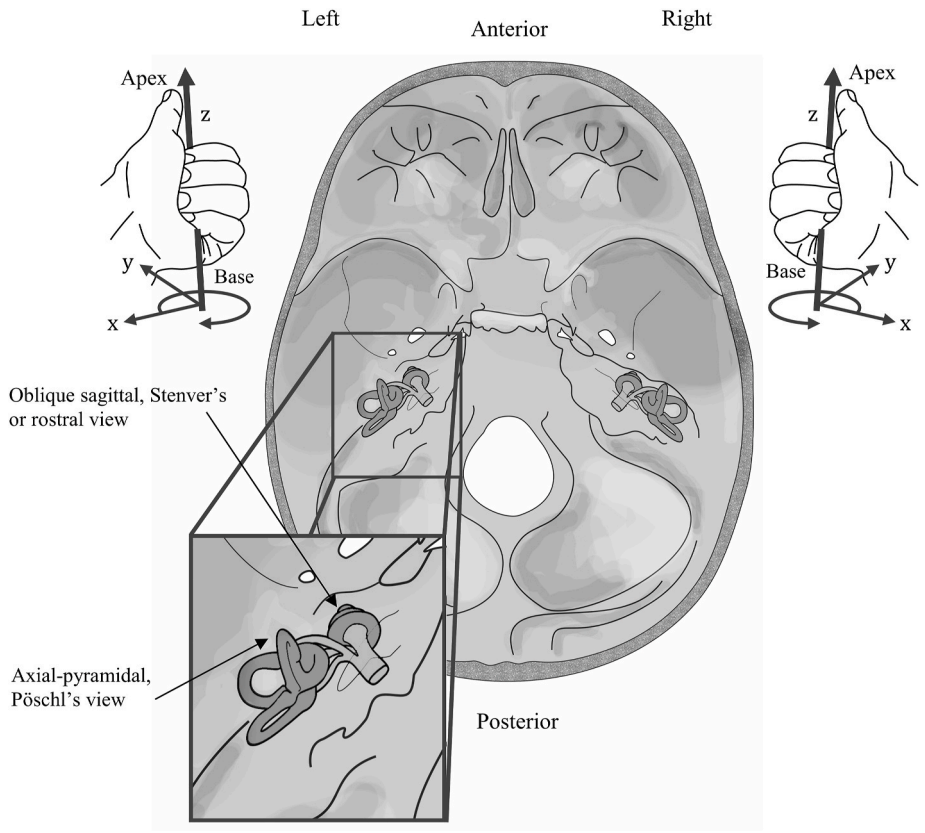

Fig. 2. A superior, *in vivo* view of the cochlea demonstrates its position and the handedness of the coordinate system for the left and right cochleae. Anatomical terminology is used to indicate the directions in the image, except for the Stenver's and Pöschl's views, which are radiological terms.

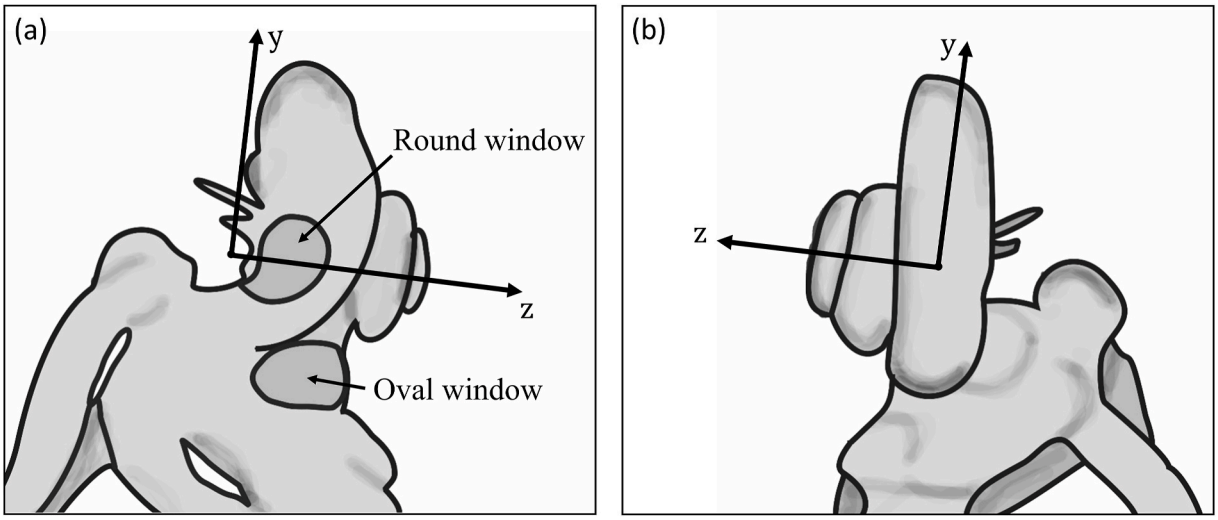

Fig. 3. (a) Round-window view of the left human cochlea where both the round and oval windows are visible. (b) The medial view of the left human cochlea is 180° from the round-window view. (Figures adapted from Pietsch, Aguirre Dávila, Erfurt, Avci, Lenarz and Kral [9]).

2.3.4. Cochlear view

The *cochlear view* is the "top view" of the cochlea [9], which in anatomical terms is also known as the *ventral* or *oblique sagittal* or *rostral view* of the cochlea as seen in Fig. 4a. The *cochlear view* is parallel to the *base plane* ($z = 0$) in the cochlear coordinate system, and is viewed from positive to negative z, as shown in Fig. 1. Radiographically, the *Stenver's view* is used to obtain a projection on a plane parallel to the long axis of the petrous bone, i.e. it is taken from the same angle as the *cochlear view*, though the field of view may differ from that of the *cochlear view* [6]. Recently, Pietsch, Schurzig, Salcher, Warnecke, Erfurt, Lenarz and Kral [10] referred to this view as the *top-axial view* or *rostral view* of the cochlea. In this view, the cochlea's apex, round window, oval window, basal turn of the cochlea, vestibule, and anterior branches of the superior and lateral semi-circular canals are visible [11]. To obtain this view from a 3D image stack, a line perpendicular to the modiolar axis is aligned to a horizontal view through the midpoint of the round window [12]. For anatomical structures visible from the intact exterior of the cochlea, e.g., when measuring a corrosion cast, the *cochlear view* may be

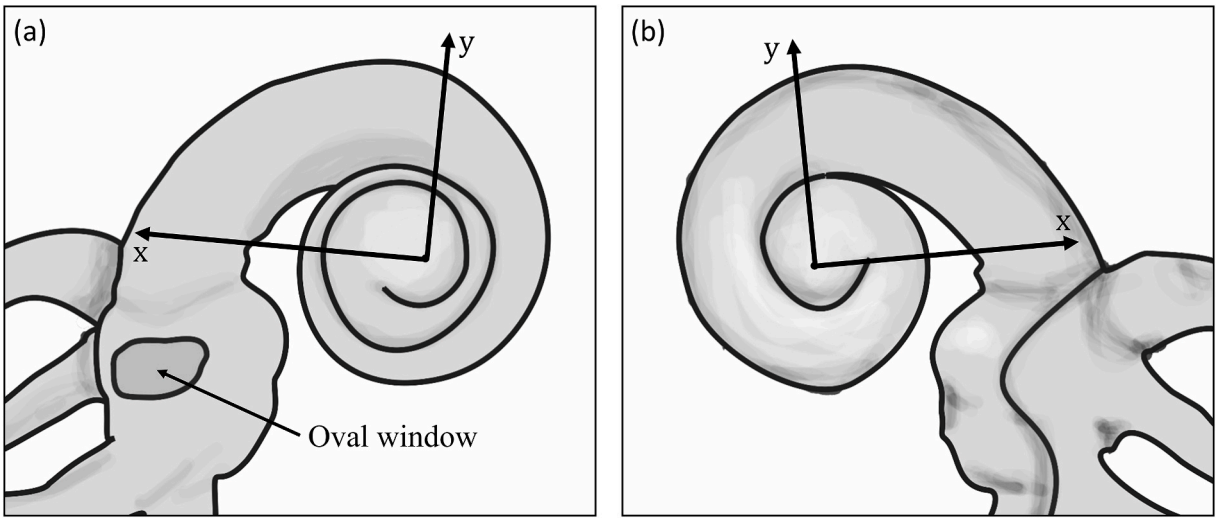

Fig. 4. (a) *Cochlear view* of the left human cochlea showing the alignment with the cochlear coordinate system. (b) *Base view* of the left human cochlea. (Adapted from Pietsch, Aguirre Dávila, Erfurt, Avci, Lenarz and Kral [9]).

used to determine length measurements along the x-axis, e.g., cochlear length (CL), or width measurements along the y-axis, e.g., cochlear width (CW).

2.3.5. Base view

The *base view* of the cochlea or *caudal, dorsal* or *basal-axial view*, as seen in Fig. 4b–is the exact opposite of the *cochlear view*. In other words, the apex of the cochlea will not be visible in this view [9,10]. There is no radiological equivalent for this view. Although the *Caldwell* and *Towne views* are obtained from the basal side of the cochlea [13], they are not exactly opposite to the *Stenver's view*. It is the same as the *bottom-axial view* on the length plane from negative z to positive z [6,14].

2.4. Mid-modiolar views and planes

A *mid-modiolar view*, as shown in Fig. 5, is a view on a plane through the modiolar axis of the cochlea. To obtain a mid-modiolar view, the cochlea must be aligned to the cochlear coordinate system, as shown in Fig. 1, after which it must be sliced radially through the z-axis, i.e. the modiolus. Slices in the ascending direction of the cochlea will follow an anticlockwise direction for right cochleae (right-handed coordinate system) or a clockwise direction for left cochleae (left-handed coordinate system) when viewed from positive to negative z. The mid-modiolar view of the xz-plane ($y = 0$; $\theta = 0°$ (*or* 180°)) is the *length plane* of the cochlea, while a mid-modiolar view of the yz-plane ($x = 0$; $\theta = 90°$ (or 270°)) is the *width plane* of the cochlea (Fig. 1).

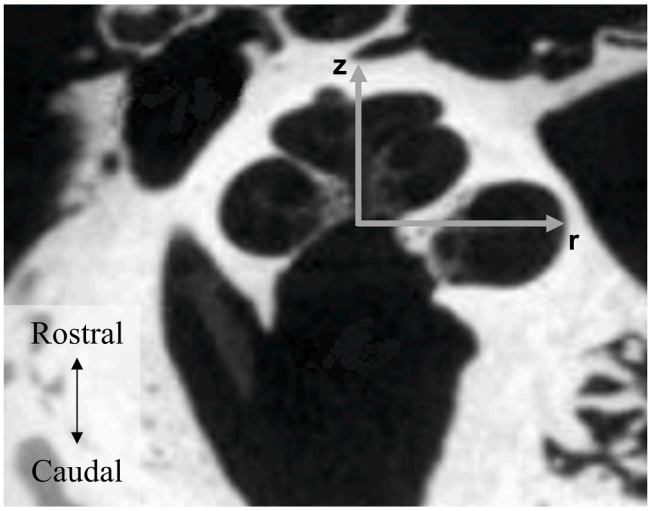

Fig. 5. *Mid-modiolar view* of the left human cochlea (μCT image) at an unspecified angle showing the z-axis aligned with the modiolus and the radius r to the lateral point of the lower basal turn.

While length measurements are by definition taken on the length plane along the x-axis, e.g., the length of the basal turn, and width measurements are by definition taken on the width plane along the y-axis perpendicular to the length measurements, the rotational angle θ of any other mid-modiolar view on which measurements are taken should be noted to provide a basis for comparison. Measurements on mid-modiolar views and planes provide both radial (r in cylindrical coordinates, where $r = \sqrt{x^2 + y^2}$ with x and y in the cartesian coordinate system) and height (z) coordinates as shown in Fig. 6. On the width plane, r = y, and on the length plane, r = x. Table 1 summarises the terminology used to describe the views of the cochlea.

2.5. Cochlear landmark standard

Computational models of the cochlea, such as those used to study the distribution of stimulation currents injected by an intracochlear electrode array [1,15–19], may be constructed with high fidelity from image sources that provide a high-resolution representation of the anatomy, e.g., morphological sections and μCT images [20]. However, these imaging techniques are unsuitable for obtaining geometric data from live cochleae due to the destructive nature thereof. Computational reconstruction of live cochleae relies on low-resolution clinical image data, which may affect the accuracy and precision of the data [3,21].

To define a measurement standard, the choice of landmarks needs to be informed by the typical structures that are included in *high-resolution* 3D computational models of the cochlear anatomy, e.g., the basilar membrane and organ of Corti [3,17]. For the reconstruction of live cochleae from *low-resolution* image data, a subset of these landmarks based on features that may be discerned on clinical images may be used. An advantage of including a complete set of landmarks in the standard is that high-resolution information about the cochlea's inner structures may be used to augment incomplete landmark sets obtained from clinical images. There is still much work to be done on deriving accurate user-specific inner structure information for live cochleae. A user-specific inner structure can potentially improve the predictions from the computational models, as it may afford a more accurate description of the location of the CI electrode array relative to the

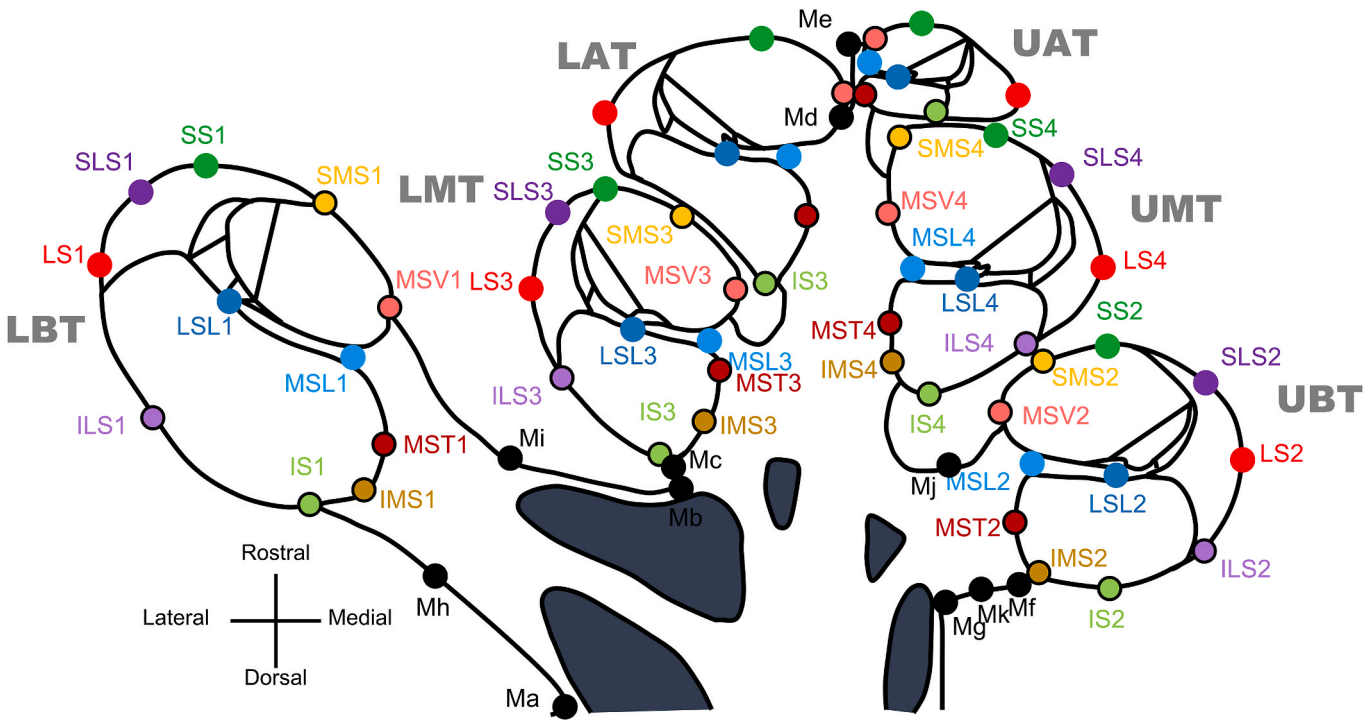

Fig. 6. Illustration of the location of the landmarks on a schematic representation of a mid-modiolar section through the human cochlea. The landmarks in the apical turn are not labelled for clarity.

Table 1
Summary of the terminology used to describe the views of the cochlea.

Standard for 3D modelling	Anatomical terminology	Radiological terminology	Clinical terminology
Round-window view	Axial-pyramidal view Lateral view	Pöschl's view	Modiolar view
Medial view	Ascending spiral view	–	Transverse view
Cochlear view	Oblique sagittal view Apex view Ventral view Top view Top-axial view Rostral view	Stenver's view	Cochlear view
Base view	Caudal view Dorsal view Basal-axial view	–	–
Mid-modiolar view[a]	Mid-modiolar view	–	–
Side view[a]	Axial-pyramidal view Lateral view	–	Modiolar view

[a] These views are taken at unspecified angles. The axial-pyramidal and lateral views are special cases of the side view where the viewing angle is known.

anatomical structures and a more accurate description of the volumetric distribution of the tissue impedances [22].

The first subset of landmarks is defined on the circumference of the cochlear canal and, when measured on subsequent mid-modiolar slices through the cochlea, describes its spiralling trajectory from base to apex. These include the lateral-most, medial-most (scala vestibuli), medial-most (scala tympani), superior-most, inferior-most, superolateral, inferolateral, superomedial and inferomedial landmarks of each turn. The spirals described by these landmarks are labelled *lateral spiral* (LS), *medial scala vestibuli* (MSV) spiral, *medial scala tympani* (MST) spiral, *superior spiral* (SS), *inferior spiral* (IS), *superolateral spiral* (SLS), *inferolateral spiral* (ILS), *superomedial spiral* (SMS) and *inferomedial spiral* (IMS), respectively. The landmarks are numbered according to the half-turn of the cochlea where they are measured, as shown in Fig. 6. The number 1 denotes the lower basal turn (LBT) starting at the round window and ending just before 180° from the round window. The number 2 denotes the upper basal turn (UBT) that spans the region from 180° to just before 360° from the round window. Likewise, 3 denotes the lower middle turn (LMT), 4 denotes the upper middle turn (UMT), 5 denotes the lower apical turn (LAT), and 6 denotes the upper apical turn (UAT), which would typically only span 90° for a total of 990° or 2.75 turns.

The importance of the cochlear canal landmark subset within the context of computational modelling of electrical stimulation of the auditory periphery is in defining the size and shape of the canal and, therefore, the volumes through which electrical stimulation currents delivered through a CI must propagate to the surviving auditory nerve fibres. The MSV and MST landmarks indicate the location of the modiolar wall, which may be used to estimate the distance between a CI electrode array and the neural elements inside the modiolus.

The second subset of landmarks describes the only internal structure visible on μCT, i.e., the spiral lamina (SL). The SL can typically not be discerned on clinical images. SL data obtained from μCT images may be used as a basis for adapting an inner structure template of the cochlea (which is typically used to add anatomical details when the resolution of image data is not sufficient to resolve these details) to reflect a measure of person-specificity in a computational model. The lateral- and medial-most points of the SL, labelled lateral spiral lamina (LSL) and medial spiral lamina (MSL), respectively, were therefore included. The same rotational sequence of landmarks through the six half-turns of the cochlea applies to describe the LSL and MSL spirals.

The third subset of landmarks describes aspects of the geometry of the modiolus. These landmarks are not rotational like the first two subsets in that they do not connect sequentially to describe the trajectory of a consistent point on the structure from base to apex. These landmarks instead indicate the extent of the modiolus along the modiolar axis and at the base of the cochlea.

Table 2 describes the cochlear landmark standard, which serves as a 3D model reconstruction framework, while Fig. 6 shows the location of the landmarks on a mid-modiolar section through the cochlea.

Table 2
Description of landmarks placed on each mid-modiolar section. For spiralling landmarks, *n* denotes the half-turn in which the landmark is located.

Abbreviation	Description
Landmarks describing the cochlear canal	
LSn	Lateral-most point
MSVn	Medial-most point on Scala Vestibuli
MSTn	Medial-most point on Scala Tympani
SSn	Superior-most point
ISn	Inferior-most point
SLSn	Superolateral spiral between LS and SS
ILSn	Inferolateral spiral between LS and IS
SMSn	Superomedial spiral between MSV and SS
IMSn	Inferolateral spiral between MST and IS
Landmarks describing the inner structure of the cochlea	
LSLn	Lateral spiral lamina
MSLn	Medial spiral lamina
Landmarks describing the shape and size of the modiolus	
Ma	Modiolar inlet below lower basal turn
Mb	Modiolar indent above LBT
Mc	Between Mb and IS2
Md	Highest point on modiolus lower turn side
Me	Highest point on modiolus higher turn side
Mf	Between Mg and IS6
Mg	Modiolar inlet below upper basal turn

2.6. Cochlear measurements standard

Table 3 details standard set of measurements for quantifying cochlear dimensions. The results section provides a summary of measurements made for visible landmarks on a data set comprising 30 μCT image stacks, while the discussion section explores each component of the standard through a comparison of the measurements made in this study and cochlear dimensions reported in the literature. Inconsistencies in measurement techniques as well as terminology relative to the proposed standard are pointed out. It is important to define and report standard set of measurements to ensure that variations in cochlear morphology are captured correctly.

2.7. Data acquisition

2.7.1. Samples and imaging

Thirty (30) cochleae from dry temporal bones and skulls were scanned at NECSA (South African Nuclear Energy Corporation), which houses the Nikon XTH 225 ST micro-focuses X-ray tomography scanner (MIXRAD), according to the procedure of Hoffman and de Beer [23]. The samples were placed in a polystyrene mould to ensure that each sample remained stable. Because of the size of the samples in this study, a spatial resolution of 90–120 μm was achieved. Each of the 2D digitized radiographs per specimen, taken at different angles, consisted of an array of 2048 x 2048-pixel elements (maximum for the current detector at the μCT system) and each element with a different grey scale (up to 65536 grey levels). Scanning parameters for the μCT scans were as follows: 33.33 min exposure time, 2 s rotation time, 100 kV tube voltage, and 100 effective mAs.

The volume files from the μCT scans were imported into VGStudioMAX-2.2 visualization software (Volume Graphics GmbH, Heidelberg, Germany) for the 3D rendering, segmentation and visualization of the reconstructed volume data (Volume Graphics, 2010).[1]

Ethical clearance for this study was obtained from the Research Ethics Committee of the Faculty of Health Sciences, University of XXX (Ethics number:174–2013). The authors wish to state that every effort was made to follow all local and international guidelines and laws that pertain to the use of human cadaveric donors in anatomical research.

[1] www.volumegraphics.com.

Table 3
Standard set of measurements for quantifying cochlear dimensions.

Measure	Abbreviation	Description	Unit	Figure
Set of measurements describing the rotational length of the cochlea				
These measurements are determined along the spiralling trajectory of the cochlear canal from base to apex, typically using the cochlear view.				
Number of turns	NT	The number of times (expressed in turns or degrees) that the cochlea circumnavigates its central axis (typically the centre of the modiolus) measured from the half diameter of the round window to the apex.	turns	7b
Angular length	AL		degrees	
Set of measurements describing the metric length of the cochlea				
These measurements are taken along the spiralling trajectory of the cochlear canal from base to apex, typically using the cochlear view.				
Lateral wall length	LWL	Measured from the half diameter of the round window to the apex along the lateral cochlear wall. This measure is the standard measure for metric length.	mm	8
Medial wall length	MWL	Measured from the half diameter of the round window to the apex along the modiolar wall.	mm	–
Measure describing the curl of the cochlea				
Wrapping factor	WF	The ratio between the angular and metric lengths.	degrees/mm	–
Set of measurements describing cochlear size				
The length and width measurements are taken on the outer boundaries of the cochlea, typically using the cochlear view.				
Cochlear length	CL or A	The dimension taken from the middle of the round window through the central axis of the cochlea to the opposite cochlear wall of the basal turn.	mm	8
Cochlear width	CW or B	The dimension perpendicular to that of the CL taken through the modiolar axis between the outer walls of the basal turn.	mm	8
The height of the cochlea may be measured on the length plane or the width plane of the cochlea. Measurements taken on the length plane are indicated with a postscript L, while measurements taken on the width plane of the cochlea are indicated with a postscript W.				
Total height on length plane	THL	The measure taken between the most superior boundary to the most inferior boundary of the cochlea parallel to the modiolar axis on the length plane of the cochlea.	mm	8
Total height on width plane	THW or H	The maximum internal diameter of the basal turn parallel to the modiolar axis on the width plane of the cochlea.	mm	8
Set of measurements describing the internal structure of the cochlea				
Length measurements are taken on the length plane of the cochlea, and width measurements are taken on the width plane of the cochlea.				

(*continued on next page*)

Table 3 (*continued*)

Measure	Abbreviation	Description	Unit	Figure
Lengths and widths of the turns				
Length/width of the basal/middle/apical turn	L/WBT L/WMT L/WAT	The dimension from the lateral-most point of the lower basal/middle/apical turn to the lateral-most point of the upper basal/middle/apical turn on the length/width plane of the cochlea.	mm	8
Height of the turns				
Height of the basal/middle/apical turn on the length/width plane	$HBL/W_{L/U}$ $HML/W_{L/U}$ $HAL/W_{L/U}$	The maximum height of the basal/middle/apical turn parallel to the modiolar axis on the cochlear length/width plane. The subscript L or U indicates the relative angle, i.e. lower (towards basal) or upper (towards apex) of the measure on a mid-modiolar or side view.	mm	9
Diameter of the canal and scalae				
Vertical diameter of the ST/SV	$ST\varnothing_{V\theta}$ $SV\varnothing_{V\theta}$	The maximum vertical diameter of the ST and SV. θ denotes the rotational angle at which the measure is reported.	mm	10
Horizontal diameter of the ST/SV	$ST\varnothing_{H\theta}$ $SV\varnothing_{H\theta}$	The maximum horizontal diameter of the ST and SV. θ denotes the rotational angle at which the measure is reported.	mm	
Vertical diameter of the cochlear canal	$C\varnothing_{V\theta}$	The total vertical internal diameter of the bony canal. θ denotes the rotational angle at which the measure is reported.	mm	10
Horizontal diameter of the cochlear canal	$C\varnothing_{H\theta}$	The total horizontal internal diameter of the bony canal. θ denotes the rotational angle at which the measure is reported.	mm	
Taxonomic classification of the cochlea				
Rollercoaster		>0.3 mm dip at start of lower basal turn; vertical jump in upper basal turn.	–	–
Intermediate		Vertical jump in upper basal turn.	–	–
Sloping		No pronounced features; approximately monotonous increase in vertical trajectory.	–	–

2.7.2. Orientation of image data and manual digitization of landmarks

Each cochlea was orientated in the *cochlear view* according to the method described by Verbist, Skinner, Cohen, Leake, James, Boëx, Holden, Finley, Roland, Roland, Haller, Patrick, Jolly, Faltys, Briaire and Frijns [8]. Landmarks were mapped on the mid-modiolar sections of each cochlea using the multipoint measuring tool in Image J.[2]

The landmarks in Table 2 were digitized on 36 complete mid-modiolar sections, separated by 5° and corresponding to a rotation of 180° to describe the full trajectory of a point along the length of the cochlea. The 5°-measurement interval allows for a maximum sampling distance of approximately 0.5 mm on the most lateral point of the cochlea relative to the modiolus.[3] Measurements were taken by an anatomist experienced in quantifying the cochlear landmarks in Fig. 6, to minimise observer error.

3. Results

The measurements derived from the chosen landmarks given in Table 3 are presented in Table 4. For each measurement, the mean, standard deviation and range was calculated.

AL was similar to that reported in the literature where μCT was used, even though the method used to determine AL differed among the various studies. Likewise, LWL or metric length of the cochlea measured along the lateral cochlear wall from the half diameter of the round window to the apex seems to be relatively independent of the source (histological sections, CT scans and cochlear casts) with this study's results being consistent with reported values. WF was comparable to the findings in another study where μCT scans and casts were used. Cochlear length or measurement A as well as cochlear width or measurement B were found to be similar to studies where μCT was used but larger than studies where CT scans were used. The same observation holds for the measurement for total cochlear height or measurement C and the width and length of the basal and middle turn. The height of the basal and middle turn in our study was larger than measurements reported in the literature, but may be affected by the angle at which the measurements in the literature were taken relative to the specific angles used in the

Table 4
Results (mean, standard deviation and range) of the measurements.

Measure	Abbreviation	Result
Angular length	AL	991.48 ± 44.20° (912.00–1078.00°)
Lateral wall length	LWL	42.20 ± 1.97 mm (39–45 mm)
Wrapping factor	WF	23.71 ± 1.13°/mm
Cochlear length	CL or A	9.52 ± 0.35 (8.80–10.20 mm)
Cochlear width	CW or B	7.08 ± 0.27 mm (6.32–7.50 mm)
Total height on length plane	THL	4.28 ± 0.44 mm (3.40–5.30 mm)
Total height on width plane	THW or H	4.05 ± 0.34 mm (3.20–4.50 mm)
Length of the basal/middle/apical turn	LBT LMT	9.52 ± 0.35 mm (8.8–10.2 mm) 4.37 ± 0.27 mm (3.8–5.2 mm)
Width of the basal/middle/apical turn	WBT WMT	7.07 ± 0.28 mm (6.3–7.5 mm) 3.96 ± 0.23 mm (3.40–4.30 mm)
Height of the basal and middle turn on the width plane	HBWL HMWL	2.08 ± 0.14 mm (1.80–2.30 mm) 1.96 ± 0.17 mm (1.70–2.40 mm)
Horizontal diameter of the ST	STØHθ	1.15 mm
Horizontal diameter of the cochlear canal (SV/SM)	CØHθ	0.89 mm
Rollercoaster		n = 18
Intermediate		n = 5
Sloping		n = 7

[2] https://imagej.nih.gov/ij/.

[3] Calculation based on the lateral spiral of a cochlea with a cochlear length of 12 mm.

present study. Measures of horizontal cochlear canal diameters at a rotational angle of 90° were smaller than those reported in the literature. In the present study, the rollercoaster cochlear class occurred most frequently.

4. Discussion

4.1. Measurements describing the rotational length of the cochlea

Different methods are used to determine the number of turns or angular length e.g., Pietsch, Aguirre Dávila, Erfurt, Avci, Lenarz and Kral [9] calculated angular length by performing linear regression between the width and length of the cochlear base. Biedron, Westhofen and Ilgner [24] determined the angular length histologically on a mid-modiolar section by counting the number of scala media sections with reference to the *cochlear view* as illustrated in Fig. 7a. Variation, which may in part be attributed to the different methods to determine this measure or the source of the cochlea to be measured, e.g., CT scans, μCT scans, histological sections or casts of the cochlea, is evident. The overall average number of turns among the reports captured in Table 5 is 2.63 turns (947°). The higher-resolution imaging modalities (histology and μCT) showed more turns when compared to casts and CT's.

To calculate angular length from cochlear casts, researchers have divided the cochlea into quadrants by two construction lines i.e., a line from the middle of the round window through the central axis and a second line orthogonal to the first one through the central axis [5,14]. The number of quadrants is counted to determine the number of turns as seen in Fig. 7b.

Another method to determine the number of turns is by determining the angle between the starting line of the cochlea ($\theta = 0°$) and another line from the central axis of the cochlea to the terminal point of the apical turn as demonstrated in Fig. 7b [27].

In the present study the number of turns was determined using the method described by Shin, Lee, Kim, Yoo, Shin, Song and Koh [27]. The methods by all the studies reported here conform to the standard. Here variation is rather a function of the image source that dictates the method that can be used.

4.2. Measurements describing the metric length of the cochlea

Lateral wall length (LWL) as illustrated by the dashed line in Fig. 8, is the metric length of the cochlea measured along the lateral cochlear wall from the half diameter of the round window to the apex [29,30]. This measure is sometimes referred to as cochlear length, e.g., by Pietsch, Aguirre Dávila, Erfurt, Avci, Lenarz and Kral [9]. LWL was defined by Kawano, Seldon and Clark [26] as the outer wall length along the scala tympani, which might not exactly correspond to the LWL determined from corrosion casts as the lateral-most point of the cochlear canal might not always be aligned with the scala tympani.

One technique to measure LWL is described by Erixon, Högstorp, Wadin and Rask-Andersen [5] where the cochlea is divided into four quadrants by lines drawn from the midpoint of the round window through the central axis to the opposite wall (i.e. a line along the length axis) and a second orthogonal line drawn to the first line (i.e. a line on the width axis). The length of the outer wall of each segment is determined and summed to determine the LWL of the cochlea. A spiral function that provides a good fit to the path of the entire outer wall from base to apex without requiring multiple sections of simple or logarithmic spirals was used by Xu, Xu, Cohen and Clark [31] and Yoo, Ge, Rubinstein and Vannier [32] to model the line tracing the outer wall of the cochlea. The LWL was determined by Pietsch, Aguirre Dávila, Erfurt, Avci, Lenarz and Kral [9] by creating individualised 3D representations of the lateral wall for 108 corrosion casts using a regression scaling model for the lateral wall by using two input parameters, i.e. the cochlear length and cochlear width. Hussain, Frater, Calixto, Karoui, Margeta, Wang, Hoen, Delingette, Patou, Raffaelli, Vandersteen and Guevara [30] used the web-based Oticon Medical Nautilus software [33] to determine LWL on 1099 CT scans of cochleae and referred to this measure as cochlear duct length.

The metric length of the cochlea is often measured at the level of the basilar membrane to allow application of Greenwood's function [34] to determine the frequency map for a particular cochlea. For example, Ketten, Skinner, Wang, Vannier, Gates and Gail Neely [35] and Skinner, Ketten, Holden, Harding, Smith, Gates, Neely, Kletzker, Brunsden and Blocker [36] approximated the location of the basilar membrane on high-resolution CT images at the centroid of the fluid space of the cochlear canal and calculated the length of the basilar membrane by fitting an Archimedean spiral equation to individual cochleae. These authors also referred to the metric length as cochlear length. To allow comparison among metric length measurements from different studies, it is important to note the location at which such a measure was determined relative to the cochlear structures. The studies by Ketten, Skinner,

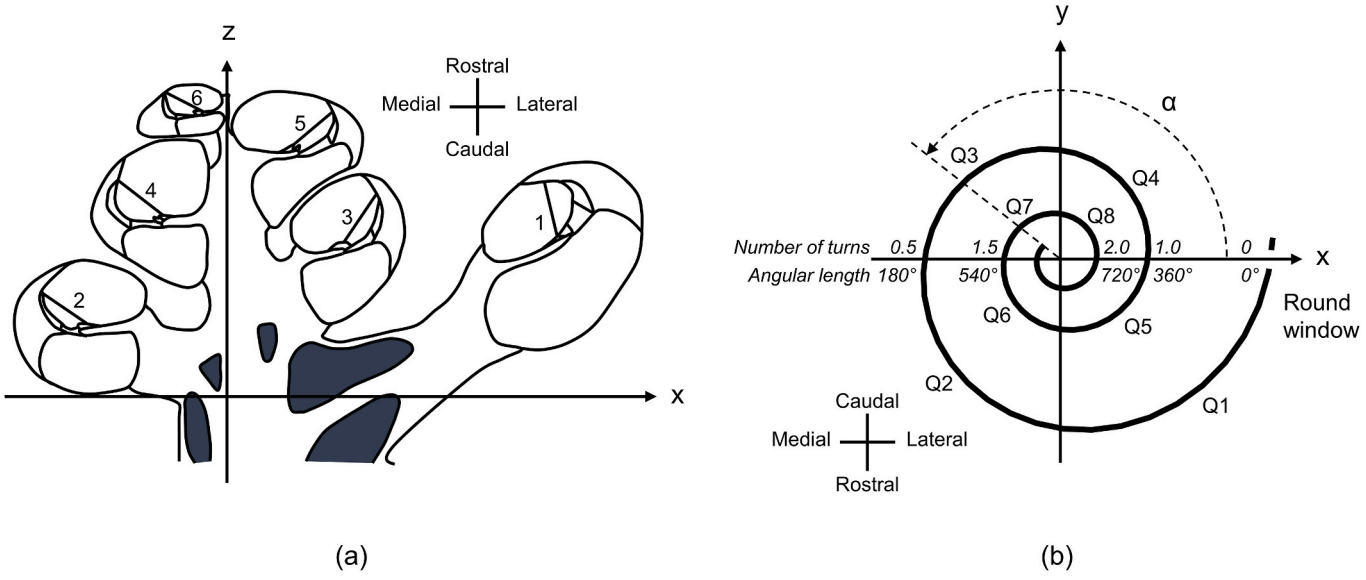

Fig. 7. (a) Histologic method of Biedron, Westhofen and Ilgner [24] to determine angular length. (b) The number of turns is determined on cochlear casts by counting quadrants indicated by Q1 to Q1 [5] or by measuring the angle α of the terminal point of the apical turn (helicotrema) [27].

Table 5
Reported measures of rotational length in the literature compared to our data.

Study	Method	Population group	n	m	Number of turns, classification or Mean ± SD (Range)	Angular length (°), classification or Mean ± SD (Range)
Kawano, Seldon and Clark [26]	Histology	Japanese	84		2.69 ± 0.11 turns	968.4° ± 40°
Tian, Linthicum and Fayad [28]	Histology		9	6	2.5 turns	900°
				3	3 turns	1080°
Biedron, Westhofen and Ilgner [24]	Histology	German	157	2	NT < 2.50	AL < 900°
				54	NT = 2.50	AL = 900°
				84	2.50< NT ≤ 2.75	900° < AL ≤ 990°
				17	2.75< NT < 3.00	990° < AL < 1080°
Erixon, Högstorp, Wadin and Rask-Andersen [5]	Casts	Swedish	73		2.60 turns (2.20–2.90 turns)	929° (774°–1037°)
Fernando, Jesus, Opulencia, Maglalang and Chua [25]	CT	Filipino	194	179	2.5 turns	900°
				15	2.75 turns	990°
Shin, Lee, Kim, Yoo, Shin, Song and Koh [27]	µCT	Korean	39		2.54 ± 0.09 turns (2.36–2.80 turns)	850.70° (916.20°–1007.70°)
Pietsch, Aguirre Dávila, Erfurt, Avci, Lenarz and Kral [9]	Casts	German	108		2.68 - 2.7 turns	956 ± 40°
	µCT		30			967 ± 45°
Present study	µCT	South African	30		2.78 ± 0.14 turns (2.41–2.99 turns)	991.48 ± 44.20° (912.00–1078.00°)

n: Sample size, m: Sample subset in category, SD: Standard deviation, µCT: Micro-computed tomography, CT: Computed tomography.

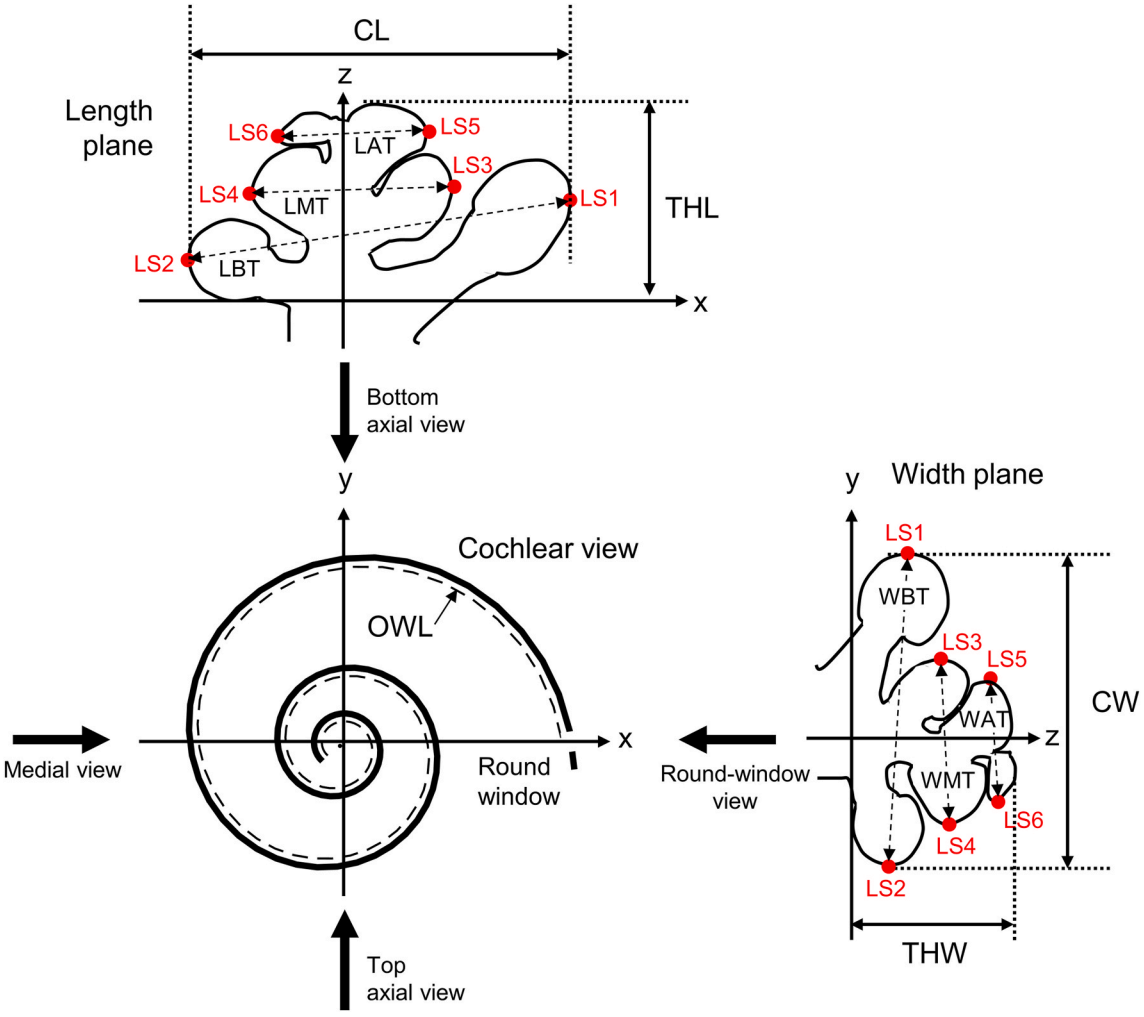

Fig. 8. Illustration of LWL as determined along the lateral cochlear wall as well as length, width and height measurements taken on the length and width planes. CL is the A parameter, CW is the B parameter and THW is typically the H parameter defined in the literature [9]. (LWL: lateral wall length, CL: cochlear length, CW: cochlear width, THW: Total height of cochlea on width plane).

Wang, Vannier, Gates and Gail Neely [35] and Skinner, Ketten, Holden, Harding, Smith, Gates, Neely, Kletzker, Brunsden and Blocker [36], for example, give metric lengths of 33.01 ± 3.31 mm (n = 20) and 34.62 ± 1.22 mm (n = 13) respectively, which, except for the study by Escudé, James, Deguine, Cochard, Eter and Fraysse [37], is lower than the values reported for LWL (Table 6) because the measure was taken at a landmark closer to the modiolus.

Table 6
Reported measures of LWL in the literature compared to our data.

Study	Method	Population group	n	Mean ± SD (Range)
Sato, Sando and Takahashi [50]	Histology	American	18	38.64 ± 3.19 mm (32.70–43.20 mm)
Kawano, Seldon and Clark [26]	Histology	Japanese	8	40.81 ± 1.97 mm (37.93–43.81 mm)
Escudé, James, Deguine, Cochard, Eter and Fraysse [37]	CT	French	42	34.40 ± 2.20 mm (30.76–37.41 mm)
Erixon, Högstorp, Wadin and Rask-Andersen [5]	Casts	Swedish	58	42.00 ± 1.96 mm (38.60–45.60 mm)
Erixon and Rask-Andersen [29]	Casts	Swedish	51	41.20 ± 1.86 mm (37.60–44.90 mm)
Würfel, Lanfermann, Lenarz and Majdani [51]	CBCT	German	436	37.90 ± 1.98 mm (30.80–43.20 mm)
Pietsch, Aguirre Dávila, Erfurt, Avci, Lenarz and Kral [9]	Casts μCT	German	108 30	(36.00–46.00 mm)
Hussain, Frater, Calixto, Karoui, Margeta, Wang, Hoen, Delingette, Patou, Raffaelli, Vandersteen and Guevara [30]	CT	European	1099	M: 41.48 ± 1.06 mm F: 41.07 ± 0.91 mm
Present study	μCT	South African	30	42.20 ± 1.97 mm (39–45 mm)

n: Sample size, SD: Standard deviation, μCT: Micro computed tomography, CT: Computed tomography, M: Male, F: Female.

4.3. Measure describing the curl of the cochlea

The tightness of the curl of a cochlea has implications for intracochlear electrode location for non-lateral wall electrode arrays and may also affect electrode insertion trauma during surgical placement of the array. Pietsch, Aguirre Dávila, Erfurt, Avci, Lenarz and Kral [9] defined the WF as the ratio between AL and LWL to provide a measure of the tightness with which the cochlea curls around the modiolus. According to Pietsch, Aguirre Dávila, Erfurt, Avci, Lenarz and Kral [9] a high wrapping was observed in cochleae with a small base. Wrapping factors reported vary, e.g., Pietsch, Aguirre Dávila, Erfurt, Avci, Lenarz and Kral [9] reported values of between 21 and 27°/mm, while Hussain, Frater, Calixto, Karoui, Margeta, Wang, Hoen, Delingette, Patou, Raffaelli, Vandersteen and Guevara [30] reported wrapping factors of around 81°/mm which suggests that an alternative metric length measure than LWL was used to calculate their WF. Another common definition for WF is the ratio of the active length of the electrode array (from the most basal to the most apical electrode contact) and the length along the lateral wall of the ST as a measure of how tightly an intracochlear electrode array is wrapped around the modiolus [38]. The measure approaches 1.0 if the electrode is located along the lateral wall and decreases as the electrode approaches the modiolar wall. Care must be taken to distinguish between the anatomical and electrode interpretations of WF.

Table 7 shows nearly identical WFs reported from the present study and that of Pietsch, Aguirre Dávila, Erfurt, Avci, Lenarz and Kral [9], suggesting that WF is robust against measurements from at least corrosion casts and μCTs.

Table 7
Reported measures of anatomical WF in the literature compared to our data.

Study	Method	Population group	n	Mean ± SD
Pietsch, Aguirre Dávila, Erfurt, Avci, Lenarz and Kral [9]	Casts μCT	German	108 30	23.7 ± 1.2°/mm
Present study	μCT	South African	30	23.71 ± 1.13°/mm

n: Sample size, SD: Standard deviation, μCT: Micro computed tomography.

4.4. Measurements describing cochlear size

Inconsistent terminology is common when measurements of the length and width of the cochlea are reported. The standard proposed in this article denotes the terminology according to the mid-modiolar plane through the cochlea on which measurements are taken as shown in Fig. 8.

4.4.1. Cochlear length

Cochlear length or the parameter *A*, is defined as the dimension taken from the middle of the round window through the central axis of the cochlea to the opposite cochlear wall when the cochlea is positioned in the cochlear view [11,37,39] as illustrated in Fig. 8. It is important to note that CL is not the same as the length of the basal turn (LBT), the latter being measured on the length plane of the cochlea when viewing from the top or bottom-axial views, i.e., at an angle perpendicular to the round-window view as seen in Fig. 8. Martinez-Monedero, Niparko and Aygun [6] and Avci, Nauwelaers, Lenarz, Hamacher and Kral [14], referred to CL as the *length of the base of the cochlea*. Similarly, Pietsch, Aguirre Dávila, Erfurt, Avci, Lenarz and Kral [9] use the term *cochlear base length* for CL while Escudé, James, Deguine, Cochard, Eter and Fraysse [37] referred to this measure simply as A.

Dimopoulos and Muren [4] defined CL as the transverse diameter drawn from a point just in front of the round window in the Stenver's view. Pietsch, Schurzig, Salcher, Warnecke, Erfurt, Lenarz and Kral [10] determined CL (referred to as the A-axis) on corrosion casts and clinical CT from the round window to the opposite wall. Avci, Nauwelaers, Lenarz, Hamacher and Kral [14] calculated the dimension by starting at the inferior edge of the round window, measuring CL by the summation of two constructive lines with the cochlea orientated in the cochlear view. The first line was drawn from the midpoint of the round window to the modiolar axis, while the second line was an extension of the first from the modiolar axis to a distant point on the first turn. Ketten, Skinner, Wang, Vannier, Gates and Gail Neely [35] and Skinner, Ketten, Holden, Harding, Smith, Gates, Neely, Kletzker, Brunsden and Blocker [36] reported CL as *basal diameter*, though their measurements were taken between landmarks at the centroid of the fluid space of the cochlea, approximately at the LSL landmark in Fig. 6. Their length measurements, 7.91 ± 0.53 mm (n = 20) and 8.01 ± 0.3 mm (n = 13) respectively, are consequently smaller than those reported in the literature.

The average CL reported by researchers in Table 8 is 9.08 mm.

4.4.2. Cochlear width

Cochlear width or the parameter *B*, is the dimension perpendicular to CL between the opposite cochlear walls in the base when the cochlea is orientated in the cochlear view. This measurement is taken on the width axis as illustrated in Fig. 8. As for CL, one should note that the width of the basal turn (WBT) is not the same as the CW. The dimension is sometimes referred to as the *vertical height of the basal turn* [4]. Other authors described this measure as the *width of the basal turn measured orthogonally to the CL* [5,6,14]. Pietsch, Aguirre Dávila, Erfurt, Avci, Lenarz and Kral [9] refers to the width of the basal turn as the *cochlear base width*.

The average CW from the studies in Table 9 is 6.93 mm. As seen in

Table 8
Reported measures of CL or A in the literature compared to our data.

Study	Method	Population group	n	Mean ± SD (Range)]
Dimopoulos and Muren [4]	Casts	Swedish	95	8.58 ± 0.45 mm (7.00–9.80 mm)
Escudé, James, Deguine, Cochard, Eter and Fraysse [37]	CT	French	42	9.23 ± 0.53 mm (7.9–10.8 mm)
Krombach, van den Boom, Di Martino, Schmitz-Rode, Westhofen, Prescher, Günther and Wildberger [52]	CT	German	120	R = 9.12 ± 0.60 mm (8.10–10.40 mm) L = 9.11 ± 0.60 mm (8.00–10.10 mm)
Erixon, Högstorp, Wadin and Rask-Andersen [5]	Casts	Swedish	51	9.30 mm
Fernando, Jesus, Opulencia, Maglalang and Chua [25]	CT	Filipino	388	R = 7.55 mm L = 7.60 mm
Martinez-Monedero, Niparko and Aygun [6]	CT	American	124	8.49 ± 0.60 mm (6.80–10.30)
Shin, Lee, Kim, Yoo, Shin, Song and Koh [27]	µCT	Korean	39	9.70 mm
Avci, Nauwelaers, Lenarz, Hamacher and Kral [14]	µCT	German	16	9.20 ± 0.40 mm
Avci, Nauwelaers, Hamacher and Kral [53]	µCT	German	10	9.35 ± 0.31 mm (9.00–10.03 mm)
Pietsch, Aguirre Dávila, Erfurt, Avci, Lenarz and Kral [9]	µCT Casts	German	108 30	9.30 ± 0.30 mm 9.20 ± 0.40 mm
Zahara, Dewi, Aboet, Putranto, Lubis and Ashar [11]	CT	Indonesian	36	8.75 ± 0.31 mm (8.17–9.33 mm)
Hussain, Frater, Calixto, Karoui, Margeta, Wang, Hoen, Delingette, Patou, Raffaelli, Vandersteen and Guevara [30]	CT	European	1099	M = 9.11 ± 0.58 mm F = 8.97 ± 0.52 mm
Present study	µCT	South African	30	9.52 ± 0.35 (8.80–10.20 mm)

n: Sample size, SD: Standard deviation, µCT: Micro computed tomography, CT: Computed tomography, M: Male, F: Female, L: Left, R: Right.

Table 9, high-resolution images generally resulted in a larger width of the basal and middle turns when compared to casts and CT scans.

4.4.3. Total height of the cochlea

Total *height of the cochlea* or cochlear axis height or the *H* parameter is measured from the cochlear base to the apex along the modiolar axis on a mid-modiolar view of the cochlea [9,11,14,25,26,36]. If the cochlear base is taken as a landmark in the modiolar region of the cochlear inlet [14], there may be some variation in measurements as the parameter has to be estimated by an observer, while landmarks on the canal boundaries, e.g. Fernando, Jesus, Opulencia, Maglalang and Chua [25], may provide more consistent measurements among different observers. Total cochlear height has also been calculated by the summation of the visible heights of the basal, middle and apical turns on a side view of the cochlea [5,40]. The term *axial diameter* has also been used to refer to the height of the modiolus from the base of the cochlea to the helicotrema [4]. In the present study, the total height of the cochlea was taken in the length plane (THL) and width plane (THW) between the lowest IS and the highest SS landmark, parallel to the modiolar axis as shown in Fig. 8. In the literature, researchers do not always record whether total cochlear height was taken in the length or width plane. Measurement on the different planes will inevitably differ somewhat.

The average total cochlear height for the studies in Table 10, is 4.26 mm. Again, imaging modalities with higher resolutions tend to result in greater cochlear height measurements, which might be explained by the apical turn that is obscured in lower resolution imaging modalities.

Table 9
Reported measures of CW or B compared to our data.

Study	Method	Population group	n	Mean ± SD (Range)
Dimopoulos and Muren [4]	Casts	Swedish	95	6.77 ± 0.35 mm (6.00–7.50 mm)
Escudé, James, Deguine, Cochard, Eter and Fraysse [37]	CT	French	42	6.99 ± 0.37 mm
Martinez-Monedero, Niparko and Aygun [6]	CT	American	124	6.42 ± 0.56 mm (5.20–7.80 mm)
Shin, Lee, Kim, Yoo, Shin, Song and Koh [27]	µCT	Korean	39	7.00 mm
Avci, Nauwelaers, Lenarz, Hamacher and Kral [14]	µCT	German	16	7.00 ± 0.30 mm
Avci, Nauwelaers, Hamacher and Kral [53]	µCT	German	10	7.04 ± 0.34 mm (6.71–7.63 mm)
Pietsch, Aguirre Dávila, Erfurt, Avci, Lenarz and Kral [9]	µCT Casts	German	108 30	7.00 ± 0.30 mm 6.80 ± 0.40 mm
Zahara, Dewi, Aboet, Putranto, Lubis and Ashar [11]	CT	Indonesian	36	6.53 ± 0.35 mm (5.73–7.50 mm)
Hussain, Frater, Calixto, Karoui, Margeta, Wang, Hoen, Delingette, Patou, Raffaelli, Vandersteen and Guevara [30]	CT	European	1099	M = 6.85 ± 0.25 mm F = 6.73 ± 0.21 mm
Present study	µCT	South African	30	7.08 ± 0.27 mm (6.32–7.50 mm)

n: Sample size, SD: Standard deviation, µCT: Micro computed tomography, CT: Computed tomography, M: Male, F: Female.

4.5. Measurements describing the detail structure of the cochlea

4.5.1. Lengths and widths of the cochlear turns

The *lengths of the basal, middle, and apical turns* (LBT, LMT and LAT respectively), are taken in the cochlear length plane while the corresponding width measurements, WBT, WMT and WAT are taken on the width plane (or on side views corresponding to the plane views) as shown in Fig. 8. These measurements need not be orthogonal to the modiolar axis as they are determined between the LS landmarks on opposite canal walls in the same turn on a side or mid-modiolar view of the cochlea [5]. In some cases, however, the extent of the canals has been reported along lines perpendicular to the modiolar axis [27]. These perpendicular measurements may not exactly coincide with LBT, LMT and LAT and may be expected to be somewhat smaller than the oblique measurements. However, LBT and CL are frequently very similar because the basal turn typically oriented perpendicular to the modiolar axis in studies where the morphology of the cochlea is quantified. No values have been found for medial canal lengths, though LBT and CL are often equated. Values determined in our study are given in Table 11.

The extent of the cochlear canals is typically measured on the width plane. Findings of the present study compared to those in the literature are given in Table 12.

4.5.2. Height of the cochlear turns

The *heights of the basal, middle, and apical turn* are taken parallel to the modiolar axis [5,40] typically from a side view of the cochlea where the internal structures are not visible (Fig. 9). This means that reported heights of the turns may not reflect the full internal vertical diameter of

Table 10
Reported measures of total height of the cochlea compared to our data. The measurement plane is indicated if it could be determined.

	Study	Method	Population group	n	Mean ± SD (Range)
	Dimopoulos and Muren [4]	Casts	Swedish	95	3.93 ± 0.40 mm (3.10–5.00 mm)
	Fernando, Jesus, Opulencia, Maglalang and Chua [25]	CT	Filipino	388	R = 4.36 mm (3.30–5.10 mm) L = 4.34 mm (3.40–5.20 mm)
	Avci, Nauwelaers, Lenarz, Hamacher and Kral [14]	µCT	German	16	4.40 ± 0.30 mm
THW	Erixon, Högstorp, Wadin and Rask-Andersen [5]	Casts	Swedish	73	3.90 ± 0.37 mm (3.30–4.80 mm)
	Braun, Böhnke and Stark [40]	µCT	German	1	4.06 mm
	Shin, Lee, Kim, Yoo, Shin, Song and Koh [27]	µCT	Korean	39	3.80 mm
	Pietsch, Aguirre Dávila, Erfurt, Avci, Lenarz and Kral [9]	µCT Casts	German	108 30	4.40 ± 0.40 mm 4.00 ± 0.20 mm
	Hussain, Frater, Calixto, Karoui, Margeta, Wang, Hoen, Delingette, Patou, Raffaelli, Vandersteen and Guevara [30]	CT	European	1099	M = 4.32 ± 0.15 mm F = 4.25 ± 0.15 mm
	Present study	µCT	South African	30	4.05 ± 0.34 mm (3.20–4.50 mm)
THL	Zahara, Dewi, Aboet, Putranto, Lubis and Ashar [11]	CT	Indonesian	36	3.26 ± 0.24 mm (2.80–3.72 mm)
	Present study	µCT	South African	30	4.28 ± 0.44 mm (3.40–5.30 mm)

n: Sample size, SD: Standard deviation, µCT: Micro computed tomography, CT: Computed tomography, M: Male, F: Female L: Left, R: Right.

the cochlear canal for the middle and apical turns as these may be partially embedded into the basal turn. Furthermore, few studies report the precise orientation in which the measurements taken which make direct comparison among measurements difficult. The standard proposes specifying the angles and views used to determine these measurements, i.e., width or length planes or views, lower or upper turn on this view or the angle (refer to Table 3).

In the present study, the heights of the turns were determined as the vertical diameter of the canal (see section 3.5.3)on a mid-modiolar plane of the cochlea. These vertical diameter values as determined on the width plane for the lower basal and middle turns are reported together with height values from the literature in Table 13. The height of the lower basal turn (2.09 mm) in the present study is comparable to reported measurements, e.g., the average value of 2.1 mm reported by Erixon, Högstorp, Wadin and Rask-Andersen [5]. The height of the middle turn as reported in the literature is, as expected, smaller than the internal vertical diameter of the middle turn as determined in the present study. The average reported heights of the basal and middle turns are 1.89 mm and 1.41 mm respectively.

Table 11
Reported measures of height of the basal and middle turn compared to our data.

	Study	Method	Population group	n	Mean ± SD (Range)
HBW_L	Krombach, van den Boom, Di Martino, Schmitz-Rode, Westhofen, Prescher, Günther and Wildberger [52]	CT	German	120	1.76 ± 0.03 mm (0.90–2.20 mm)
	Erixon, Högstorp, Wadin and Rask-Andersen [5]	Casts	Swedish	73	2.10 ± 0.20 mm (1.60–2.60 mm)
	Braun, Böhnke and Stark [40]	µCT	German	1	1.90 mm
	Shin, Lee, Kim, Yoo, Shin, Song and Koh [27]	µCT	Korean	39	1.90 mm
$C\varnothing_{H90}$	Present study	µCT	South African	30	2.08 ± 0.14 mm (1.80–2.30 mm)
HMW_L	Erixon, Högstorp, Wadin and Rask-Andersen [5]	Casts	Swedish	73	1.20 ± 0.17 mm (0.80–1.60 mm)
	Braun, Böhnke and Stark [40]	µCT	German	1	1.30 mm
	Shin, Lee, Kim, Yoo, Shin, Song and Koh [27]	µCT	Korean	39	1.80 mm
$C\varnothing_{H270}$	Present study	µCT	South African	30	1.96 ± 0.17 mm (1.70–2.40 mm)

n: Sample size, SD: Standard deviation, µCT: Micro Computed Tomography, CT: Computed Tomography.

Table 12
Our measures of LBT and LMT. LAT is typically obscured on µCT images.

	Study	Method	Population group	n	Mean ± SD (Range)
LBT	Present study	µCT	South African	30	9.52 ± 0.35 mm (8.8–10.2 mm)
LMT	Present study	µCT	South African	30	4.37 ± 0.27 mm (3.8–5.2 mm)

n: Sample size, SD: Standard deviation, µCT: Micro computed tomography, CT: Computed tomography, M: Male, F: Female L: Left, R: Right.

4.5.3. *Diameter of the cochlear canal and scalae*

Considerable variation exists in determining the maximum vertical and horizontal diameters of the cochlear canal and scalae, mainly because the landmarks necessary to discern these measurements are often obscured on images of the cochlea. The orientation of the measurements, as well as the landmarks that are used to determine them, either use the modiolar axis as the vertical reference (Fig. 10a) or the plane of the spiral lamina as the horizontal reference (Fig. 10b). In Fig. 10, vertical diameters are indicated by $\varnothing_{V\theta}$ while horizontal diameters are indicated by $\varnothing_{H\theta}$ where θ denotes the rotational angle at which the measure was taken.

In the CI literature, there is generally more interest in the vertical diameters of the scalae, specifically the ST, since this measure is typically smaller than the horizontal diameters and, therefore, imposes a limit on maximum electrode diameter. Zahara, Dewi, Aboet, Putranto, Lubis and Ashar [11] determined $ST\varnothing_{V\theta}$ from CT images probably using the modiolus as reference, while Braun, Böhnke and Stark [40] determined this measure as the maximal distance perpendicular to the cochlear partition. Zrunek, Lischka, Hochmair-Desoyer and Burian [41]

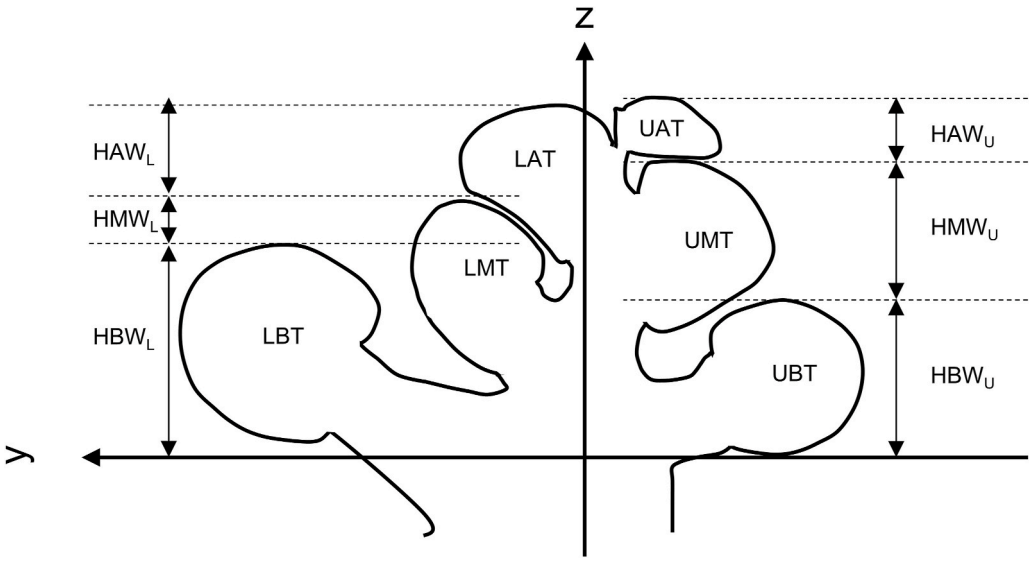

Fig. 9. Width plane showing the height of the turns on the relative lower (towards the base) and upper (towards the apex) rotational angles of the view.

Table 13
Reported measures of width of the basal and middle turns compared to our data. WAT is typically obscured on μCT images.

	Study	Method	Population group	n	Mean ± SD (Range)
WBT	Erixon, Högstorp, Wadin and Rask-Andersen [5]	Casts	Swedish	71	6.80 ± 0.46 mm (5.60–8.20 mm)
	Braun, Böhnke and Stark [40]	μCT	German	1	7.70 mm
	Present study	μCT	South African	30	7.07 ± 0.28 mm (6.3–7.5 mm)
WMT	Erixon, Högstorp, Wadin and Rask-Andersen [5]	Casts	Swedish	68	3.80 ± 0.25 mm (3.30–4.30 mm)
	Braun, Böhnke and Stark [40]	μCT	German	1	4.35 mm
	Shin, Lee, Kim, Yoo, Shin, Song and Koh [27] [a]	μCT	Korean	39	3.90 mm
	Present study	μCT	South African	30	3.96 ± 0.23 mm (3.40–4.30 mm)

n: Sample size, SD: Standard deviation, μCT: Micro Computed Tomography, CT: Computed Tomography.
[a] Measure was taken perpendicular to the modiolar axis.

used the modiolar axis as reference to determine $ST\varnothing_{V\theta}$ in relation to the diameter of two electrode arrays. Avci, Nauwelaers, Lenarz, Hamacher and Kral [14] also used the modiolar axis as reference to measure the vertical dimension of the scala tympani at lateral, central and medial locations in the scala; in this case the medial measurement would correspond to $ST\varnothing_{V\theta}$. Escudé, James, Deguine, Cochard, Eter and Fraysse [37] referred to the height of each turn as the maximal internal diameter of the cochlea from the lateral plane.

Another method that has been used to gauge the calibre of the scala tympani in relation to the diameter of electrode arrays is to determine the largest circle that could fit into the scala. This method, used by Avci, Nauwelaers, Lenarz, Hamacher and Kral [14], is a practical way to determine whether the lumen is large enough to hold an electrode array at a particular point in the cochlea.

Several researchers report dimensional variations of the ST [41–47]. Research measuring the cross-sectional diameter of the ST shows that the ST also tapers from the RW to the helicotrema, but that this is not a continuous phenomenon and may show enlargements at some places leading to even more variation and unconformity [41,42].

Braun, Böhnke and Stark [40] reported $ST'\varnothing_{H\theta}$ and $SV'\varnothing_{H\theta}$ mostly perpendicular to the cochlear partition. Givelberg and Julian [48] used the position of the centre line of the BM, its width and cross-sectional area of the scalae to create a geometric model of the cochlear anatomy while Connor, Bell, O'Gorman and Fitzgerald-O'Connor [49] constructed their model from the most distal boundary of the cochlear wall and most superior boundary of the cochlear duct. In a study by Biedron, Westhofen and Ilgner [24], the size of the scala tympani and scala vestibuli/media were measured on histological sections by matching circles to the greatest diameter of the salae using computer software. Wysocki [45] carried out a microanatomical study on 25 rubber casts of human temporal bones obtained from cadavers. These bones were dissected with the aid of an operation microscope, in which their perilymphatic spaces were filled with coloured latex and further prepared in a formalin stain. Each of the rubber moulds was removed from the osseous matrix using standard otosurgical equipment, and subsequently cut into 1 mm segments. The height and width of the vestibular and tympanic scalae were measured. To measure the internal dimensions (height, width) of the scala tympani, Avci, Nauwelaers, Lenarz, Hamacher and Kral [14] used cross-sectional images were taken every 0.1 mm orthogonal to the centerline and along the lateral wall of the ST for two cochlear turns. The slices were subsequently analyzed by custom-designed software programmed in MATLAB. The height was measured at three places namely at the center, modiolar and lateral part of each scala tympani.

It is not possible to directly determine $ST\varnothing_{V\theta}$ and $SV\varnothing_{V\theta}$ from the landmark set presented in this article, though an estimate may be derived by determining the intersection of a line parallel to the modiolar axis with the cochlear partition from IS ($ST\varnothing_{V\theta}$) or from SS ($SV\varnothing_{V\theta}$). Likewise, the present landmark set does not support direct derivation of $ST\varnothing_{H\theta}$ and $SV\varnothing_{H\theta}$ However, the total vertical diameter of the canal, $C\varnothing_{V\theta}$, may be determined as the vertical distance between IS and SS while $C\varnothing_{H\theta}$ is can be measured between the most medial of MSVS, MSL or MSTS and LS (see Table 14). Table xiv provides a summary of $C\varnothing_{H90}$ values from the literature (no values are reported for the present study). The reader is referred to specific reports in the literature for a more comprehensive overview of typical values as a function of rotational angle.

4.6. Taxonomy

The reported variations in the vertical spiralling trajectory of the cochlea have prompted researchers to attempt to classify cochleae. Erixon, Högstorp, Wadin and Rask-Andersen [5] reported cochleae that

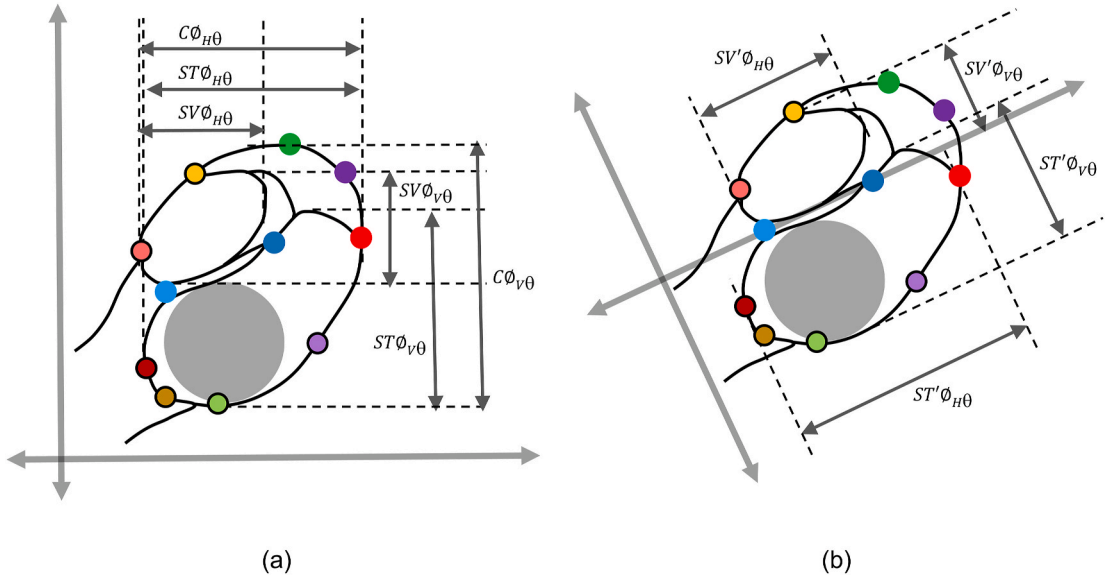

Fig. 10. The vertical ($ST\varnothing_{V\theta}$, $SV\varnothing_{V\theta}$, $C\varnothing_{V\theta}$) and horizontal ($ST\varnothing_{H\theta}$, $SV\varnothing_{H\theta}$, $C\varnothing_{H\theta}$) diameters of the ST, SV or cochlear canal are measured relative to the modiolus as vertical reference (a) or relative to the cochlear partition as the horizontal reference (b). The prime in the abbreviations in (b) indicates the deviation from the standard coordinate system. The shaded circles illustrate the method to determine the calibre of the ST by fitting a circle of maximum diameter in the lumen.

Table 14
Reported measures of horizontal cochlear canal diameters at a rotational angle of 90°.

	Study	Method	Population group	n	Mean ± SD (Range)
$C\varnothing_{H90}$	Wysocki [45]	Cadaver (rubber mould)	Polish	25	SV/SM: 1.70 mm ST: 1.50 mm
	Poznyakovskiy, Zahnert, Kalaidzidis, Lazurashvili, Schmidt, Hardtke, Fischer and Yarin [47]	CT	German	1	ST: 1.8 mm
	Braun, Böhnke and Stark [40]	µCT	German	1	SV/SM: 0.89 mm ST: 1.15 mm

n: Sample size, SD: Standard deviation, µCT: Micro Computed Tomography, CT: Computed Tomography.

had a more proximal or more distal coiling pattern. This observation was expanded by the taxonomic classification of cochleae into rollercoaster, intermediate and sloping types according to the vertical profile of the scala tympani [9,14]. Rollercoaster cochleae are characterized by a dip in the lower basal turn followed by an upward course towards the apex and a steep local increase (vertical jump) in the lower middle turn. Sloping cochleae follow a mostly monotonous upward trajectory from base to apex while the main characteristic of intermediate cochleae is, as for the roller coaster cochleae, a vertical jump in the lower middle turn.

5. Conclusion

Variation in reported measurements of cochlear dimensions originate mainly from two sources: observer error and methodological differences. Observer error is dependent on the experience and skill of the observer as well as the clarity of the source data (e.g., landmarks are more easily discernible on µCT images than on clinical CT images). While a component of observer error can be minimised by training, image clarity is often limited by the resolution and contrast of the imaging method. Methodological differences in the way that landmarks and dimensions are quantified as well as inconsistent terminology, has been shown in this article to be a major contributor to perceived variations in reported measurements. This type of error may be minimised by implementing the terminology and measurement reference proposed in this article.

Computational modelling is a valuable tool in cochlear implant research. These models are constructed from cochlear measurements, and often have to rely on reported measurements to derive landmarks and dimensions which are typically obscured on clinical images. This further accentuates the need for a well-defined, consistent framework for determining these measurements.

6. Limitations of the study

The main limitation of this study is the relatively small sample size of 30 µCT scans which were used to quantify cochlear dimensions. A larger sample size may affect the reported cochlear dimensions determined in this study. Furthermore, the history of the temporal bones, including the hearing state, ages, sexes and aetiology of the individuals is unknown which may introduce biases in the data, though this type of metadata has typically not been reported for the samples used in the studies referenced from the literature. Lastly, the measurements were taken by one observer, which may introduce observer bias. However, within the context of the article, the limitations do not affect the definition and clarification of the proposed terminology and measurement reference.

7. Ethics in publishing

The authors state that every effort was made to follow all local and international ethical guidelines and laws that pertain to the use of human cadaveric donors in anatomical research.

8. Disclosure of potential conflicts of interest

The authors declare that they have no conflict of interest.

9. Compliance with ethical standards

Ethical clearance for this study was obtained from the Research

Ethics Committee of the Faculty of Health Sciences, University of Pretoria (Ethics number:174–2013). The authors wish to state that every effort was made to follow all local and international guidelines and laws that pertain to the use of human cadaveric donors in anatomical research.

Financial interests

This work is based on the research supported in part by the National Research Foundation of South Africa (Grant number 141954). The authors have no other relevant financial or non-financial interests to disclose. All authors certify that they have no affiliations with or involvement in any organization or entity with any financial interest or non-financial interest in the subject matter or materials discussed in this manuscript.

CRediT authorship contribution statement

Rene Human-Baron: Writing – review & editing, Writing – original draft, Validation, Resources, Project administration, Methodology, Investigation, Formal analysis, Data curation, Conceptualization. **Tania Hanekom:** Writing – review & editing, Writing – original draft, Supervision, Software, Project administration, Methodology, Formal analysis, Conceptualization.

Declaration of competing interest

The authors declare that they have no known competing financial interests or personal relationships that could have appeared to influence the work reported in this paper.

.

The authors have no competing interests to declare that are relevant to the content of this article.

Acknowledgements

The authors wish to sincerely thank those who donated their bodies to science so that anatomical research could be performed. Results from such research can potentially improve patient care and increase mankind's overall knowledge. Therefore, these donors and their families deserve our highest gratitude.

References

[1] W. Badenhorst, T. Hanekom, L. Gross, J.J. Hanekom, Facial nerve stimulation in a post-meningitic cochlear implant user: using computational modelling as a tool to probe mechanisms and progression of complications on a case-by-case basis, Cochlear Implants Int. 22 (2) (2021) 68–79, https://doi.org/10.1080/14670100.2020.1824431.

[2] J. Van der Westhuizen, T. Hanekom, J.J. Hanekom, Apical reference stimulation: a possible solution to facial nerve stimulation, Ear Hear. 43 (4) (2022) 1189–1197, https://doi.org/10.1097/AUD.0000000000001170.

[3] T.K. Malherbe, T. Hanekom, J.J. Hanekom, Constructing a three-dimensional electrical model of a living cochlear implant user's cochlea, Int J Num Meth Biomed Eng 32 (7) (2016) e02751, https://doi.org/10.1002/cnm.2751.

[4] P. Dimopoulos, C. Muren, Anatomic variations of the cochlea and relations to other temporal bone structures, Acta Radiol 31 (5) (1990) 439–444, https://doi.org/10.1177/028418519003100503.

[5] E. Erixon, H. Högstorp, K. Wadin, H. Rask-Andersen, Variational anatomy of the human cochlea: implications for cochlear implantation, Otol. Neurotol. 30 (1) (2009) 14–22, https://doi.org/10.1097/MAO.0b013e31818a08e8.

[6] R. Martinez-Monedero, J.K. Niparko, N. Aygun, Cochlear coiling pattern and orientation differences in cochlear implant candidates, Otol. Neurotol. 32 (7) (2011) 1086–1093, https://doi.org/10.1097/MAO.0b013e31822a1ee2.

[7] R.W. Koch, H.M. Ladak, M. Elfarnawany, S.K. Agrawal, Measuring Cochlear Duct Length - a historical analysis of methods and results, J Otolaryngol - Head Neck Surg 46 (1) (2017) 1–11, https://doi.org/10.1186/s40463-017-0194-2.

[8] B.M. Verbist, M.W. Skinner, L.T. Cohen, P.A. Leake, C. James, C. Boëx, T. A. Holden, C.C. Finley, P.S. Roland, J.T. Roland Jr., M. Haller, J.F. Patrick, C. N. Jolly, M.A. Faltys, J.J. Briaire, J.H. Frijns, Consensus panel on a cochlear coordinate system applicable in histologic, physiologic, and radiologic studies of the human cochlea, Otol. Neurotol. 31 (5) (2010) 722–730, https://doi.org/10.1097/MAO.0b013e3181d279e0.

[9] M. Pietsch, L. Aguirre Dávila, P. Erfurt, E. Avci, T. Lenarz, A. Kral, Spiral form of the human cochlea results from spatial constraints, Sci. Rep. 7 (1) (2017) 7500, https://doi.org/10.1038/s41598-017-07795-4.

[10] M. Pietsch, D. Schurzig, R. Salcher, A. Warnecke, P. Erfurt, T. Lenarz, A. Kral, Variations in microanatomy of the human modiolus require individualized cochlear implantation, Sci. Rep. 12 (1) (2022) 5047, https://doi.org/10.1038/s41598-017-07795-4.

[11] D. Zahara, R.D. Dewi, A. Aboet, F.M. Putranto, N.D. Lubis, T. Ashar, Variations in cochlear size of cochlear implant candidates, Int. Arch. Otorhinolaryngol. 23 (2019) 184–190, https://doi.org/10.1055/s-0038-1661360.

[12] M.A. Marsh, H.A. Jenkins, N.J. Coker, Histopathology of the temporal bone following multichannel cochlear implantation, Archives oto-rhino-laryngol–Head Neck Surg 118 (11) (1992) 1257–1265, https://doi.org/10.1001/archotol.1992.01880110125022.

[13] V. Fernandes, Y. Wang, R. Yeung, S. Symons, V. Lin, Effectiveness of skull X-RAY to determine cochlear implant insertion depth, J Otolaryngol - Head Neck Surg 47 (1) (2018) 50, https://doi.org/10.1186/s40463-018-0304-9.

[14] E. Avci, T. Nauwelaers, T. Lenarz, V. Hamacher, A. Kral, Variations in microanatomy of the human cochlea, J. Comp. Neurol. 522 (14) (2014) 3245–3261, https://doi.org/10.1002/cne.23594.

[15] R.K. Kalkman, J.J. Briaire, D.M.T. Dekker, J.H.M. Frijns, Place pitch versus electrode location in a realistic computational model of the implanted human cochlea, Hear. Res. 315 (2014) 10–24, https://doi.org/10.1016/j.heares.2014.06.003.

[16] T.K. Malherbe, T. Hanekom, J.J. Hanekom, The effect of the resistive properties of bone on neural excitation and electric fields in cochlear implant models, Hear. Res. 327 (2015) 126–135, https://doi.org/10.1016/j.heares.2015.06.003.

[17] T. Hanekom, J.J. Hanekom, Three-dimensional models of cochlear implants: a review of their development and how they could support management and maintenance of cochlear implant performance, Network 27 (2–3) (2016) 67–106, https://doi.org/10.3109/0954898X.2016.1171411.

[18] J.H. Frijns, R.K. Kalkman, J.J. Briaire, Stimulation of the facial nerve by intracochlear electrodes in otosclerosis: a computer modeling study, Otol. Neurotol. 30 (8) (2009) 1168–1174, https://doi.org/10.1097/MAO.0b013e3181b12115.

[19] R.K. Kalkman, J.J. Briaire, D.M.T. Dekker, J.H.M. Frijns, The relation between polarity sensitivity and neural degeneration in a computational model of cochlear implant stimulation, Hear. Res. 415 (2022) 108413, https://doi.org/10.1016/j.heares.2021.108413.

[20] C. Bellos, G. Rigas, I.F. Spiridon, A. Bibas, D. Iliopoulou, F. Böhnke, D. Koutsouris, D.I. Fotiadis, Reconstruction of cochlea based on micro-CT and histological images of the human inner ear, BioMed Res. Int. 2014 (2014) 485783, https://doi.org/10.1155/2014/485783.

[21] A.H. Gee, Y. Zhao, G.M. Treece, M.L. Bance, Practicable assessment of cochlear size and shape from clinical CT images, Sci. Rep. 11 (1) (2021) 3448, https://doi.org/10.1038/s41598-021-83059-6.

[22] J. Thiselton, T. Hanekom, Parameterisation and prediction of intra-canal cochlear structures, Annals Biomed Eng (2024), https://doi.org/10.1007/s10439-023-03417-5.

[23] J. Hoffman, F. de Beer, Characteristics of the Micro-focus X-Ray Tomography Facility (MIXRAD) at Necsa in South Africa, 2012. https://www.ndt.net/?id=12841.

[24] J. Xu, S.-A. Xu, L.T. Cohen, G.M. Clark, Cochlear view: postoperative radiography for cochlear implantation, Otol. Neurotol. 21 (1) (2000) 49–56. PMID: 10651435.

[25] S. Biedron, M. Westhofen, J. Ilgner, On the number of turns in human cochleae, Otol. Neurotol. 30 (3) (2009) 414–417, https://doi.org/10.1097/MAO.0b013e3181977b8d.

[26] A. Fernando, B. Jesus, A. Opulencia, G. Maglalang, A. Chua, An anatomical study of the cochlea among Filipinos using high-resolution computed tomography scans, Phil J Otolaryngol Head Neck Surg 26 (2011), https://doi.org/10.32412/pjohns.v26i1.591.

[27] A. Kawano, H.L. Seldon, G.M. Clark, Computer-aided three-dimensional reconstruction in human cochlear maps: measurement of the lengths of organ of Corti, outer wall, inner wall, and rosenthal's canal, annals otol, Rhinol Laryngol 105 (9) (1996) 701–709, https://doi.org/10.1177/000348949610500906.

[28] K.-J. Shin, J.-Y. Lee, J.-N. Kim, J.-Y. Yoo, C. Shin, W.-C. Song, K.-S. Koh, Quantitative analysis of the cochlea using three-dimensional reconstruction based on microcomputed tomographic images, Anat. Rec. 296 (7) (2013) 1083–1088, https://doi.org/10.1002/ar.22714.

[29] Q. Tian, F.H. Linthicum Jr., J.N. Fayad, Human cochleae with three turns: an unreported malformation, Laryngoscope 116 (5) (2006) 800–803, https://doi.org/10.1097/01.mlg.0000209097.95444.59.

[30] E. Erixon, H. Rask-Andersen, How to predict cochlear length before cochlear implantation surgery, Acta Otolaryngol. 133 (12) (2013) 1258–1265, https://doi.org/10.3109/00016489.2013.831475.

[31] R. Hussain, A. Frater, R. Calixto, C. Karoui, J. Margeta, Z. Wang, M. Hoen, H. Delingette, F. Patou, C. Raffaelli, C. Vandersteen, N. Guevara, Anatomical variations of the human cochlea using an image analysis tool, J. Clin. Med. 12 (2) (2023), https://doi.org/10.3390/jcm12020509.

[32] S.K. Yoo, W. Ge, J.T. Rubinstein, M.W. Vannier, Three-dimensional geometric modeling of the cochlea using helico-spiral approximation, IEEE Trans. Biomed. Eng. 47 (10) (2000) 1392–1402, https://doi.org/10.1109/10.871413.

[33] J. Margeta, R. Hussain, P. López Diez, A. Morgenstern, T. Demarcy, Z. Wang, D. Gnansia, O. Martinez Manzanera, C. Vandersteen, H. Delingette, A. Buechner,

T. Lenarz, F. Patou, N. Guevara, A web-based automated image processing research platform for cochlear implantation-related studies, J. Clin. Med. 11 (22) (2022) 6640, https://doi.org/10.3390/jcm12020509.
[34] D.D. Greenwood, A cochlear frequency-position function for several species—29 years later, J Acousl Soc Am 87 (6) (1990) 2592–2605, https://doi.org/10.1121/1.399052.
[35] D.R. Ketten, M.W. Skinner, G. Wang, M.W. Vannier, G.A. Gates, J. Gail Neely, in vivo measures of cochlear length and insertion depth of nucleus cochlear implant electrode arrays, Annals Otol Rhinotol and Laryngol Suppl 175 (1998). PMID: 9826942.
[36] M.W. Skinner, D.R. Ketten, L.K. Holden, G.W. Harding, P.G. Smith, G.A. Gates, J. G. Neely, G.R. Kletzker, B. Brunsden, B. Blocker, CT-derived estimation of cochlear morphology and electrode array position in relation to word recognition in nucleus-22 recipients, J Assoc Res Otolaryngol 3 (3) (2002) 332–350, https://doi.org/10.1007/s101620020013.
[37] B. Escudé, C. James, O. Deguine, N. Cochard, E. Eter, B. Fraysse, The size of the cochlea and predictions of insertion depth angles for cochlear implant electrodes, Audiol. Neurootol. 11 (Suppl 1) (2006) 27–33, https://doi.org/10.1159/000095611.
[38] L.K. Holden, C.C. Finley, J.B. Firszt, T.A. Holden, C. Brenner, L.G. Potts, B. D. Gotter, S.S. Vanderhoof, K. Mispagel, G. Heydebrand, M.W. Skinner, Factors affecting open-set word recognition in adults with cochlear implants, Ear Hear. 34 (3) (2013) 342–360, https://doi.org/10.1097/AUD.0b013e3182741aa7.
[39] T. Khurayzi, F. Almuhawas, A. Alsanosi, Y. Abdelsamad, Ú. Doyle, A. Dhanasingh, A novel cochlear measurement that predicts inner-ear malformation, Sci. Rep. 11 (1) (2021) 7339, https://doi.org/10.1038/s41598-021-86741-x.
[40] K. Braun, F. Böhnke, T. Stark, Three-dimensional representation of the human cochlea using micro-computed tomography data: presenting an anatomical model for further numerical calculations, Acta Otolaryngol. 132 (6) (2012) 603–613, https://doi.org/10.3109/00016489.2011.653670.
[41] M. Zrunek, M. Lischka, I. Hochmair-Desoyer, K. Burian, Dimensions of the scala tympani in relation to the diameters of multichannel electrodes, Archives oto-rhino-laryngol 229 (3) (1980) 159–165, https://doi.org/10.1007/BF02565517.
[42] M. Zrunek, M. Lischka, Dimensions of the scala vestibuli and sectional areas of both scales, Archives oto-rhino-laryngol 233 (1) (1981) 99–104, https://doi.org/10.1007/BF00464279.
[43] A.P. Walby, Scala tympani measurement, annals otol, Rhinol Laryngol 94 (4) (1985) 393–397, https://doi.org/10.1177/000348948509400413.
[44] S.J. Rebscher, N. Talbot, W. Bruszewski, M. Heilmann, J. Brasell, M.M. Merzenich, A transparent model of the human scala tympani cavity, J Neurosci Meth 64 (1) (1996) 105–114, https://doi.org/10.1016/0165-0270(95)00116-6.
[45] J. Wysocki, Dimensions of the human vestibular and tympanic scalae, Hear. Res. 135 (1) (1999) 39–46, https://doi.org/10.1016/S0378-5955(99)00088-X.
[46] S.J. Rebscher, A. Hetherington, B. Bonham, P. Wardrop, D. Whinney, P.A. Leake, Considerations for design of future cochlear implant electrode arrays: electrode array stiffness, size, and depth of insertion, J. Rehabil. Res. Dev. 45 (5) (2008) 731–747, https://doi.org/10.1682/jrrd.2007.08.0119.
[47] A.A. Poznyakovskiy, T. Zahnert, Y. Kalaidzidis, N. Lazurashvili, R. Schmidt, H.-J. Hardtke, B. Fischer, Y.M. Yarin, A segmentation method to obtain a complete geometry model of the hearing organ, Hear. Res. 282 (1) (2011) 25–34, https://doi.org/10.1016/j.heares.2011.06.009.
[48] E. Givelberg, B. Julian, A comprehensive three-dimensional model of the cochlea, J Comp Phys 191 (2) (2003) 377–391, https://doi.org/10.1016/S0021-9991(03)00319-X.
[49] S.E.J. Connor, D.J. Bell, R. O'Gorman, A. Fitzgerald-O'Connor, CT and MR imaging cochlear distance measurements may predict cochlear implant length required for a 360° insertion, Am. J. Neuroradiol. 30 (7) (2009) 1425–1430, https://doi.org/10.3174/ajnr.A1571.
[50] H. Sato, I. Sando, H. Takahashi, Sexual dimorphism and development of the human cochlea: computer 3-D measurement, Acta Otolaryngol. 111 (6) (1991) 1037–1040, https://doi.org/10.3109/00016489109100753.
[51] W. Würfel, H. Lanfermann, T. Lenarz, O. Majdani, Cochlear length determination using Cone Beam Computed Tomography in a clinical setting, Hear. Res. 316 (2014) 65–72, https://doi.org/10.1016/j.heares.2014.07.013.
[52] E. Avci, T. Nauwelaers, V. Hamacher, A. Kral, Three-dimensional force profile during cochlear implantation depends on individual geometry and insertion trauma, Ear Hear. 38 (3) (2017) e168–e179, https://doi.org/10.1097/aud.0000000000000394.
[53] G.A. Krombach, M. van den Boom, E. Di Martino, T. Schmitz-Rode, M. Westhofen, A. Prescher, R.W. Günther, J.E. Wildberger, Computed tomography of the inner ear: size of anatomical structures in the normal temporal bone and in the temporal bone of patients with Menière's disease, Europ Radiol 15 (8) (2005) 1505–1513, https://doi.org/10.1007/s00330-005-2750-9.